HHS Public Access

Author manuscript

Gene Ther. Author manuscript; available in PMC 2011 July 01.

Published in final edited form as:

Gene Ther. 2011 January ; 18(1): 43–52. doi:10.1038/gt.2010.105.

Robust Cardiomyocyte-Specific Gene Expression Following Systemic Injection of AAV: In Vivo Gene Delivery Follows a Poisson Distribution

Konkal-Matt R. Prasad, PhD[1], **Yaqin Xu, MD, PhD**[1], **Zequan Yang, MD, PhD**[1], **Scott T. Acton, PhD**[3], and **Brent A French, PhD**[1,2]

[1] Department of Biomedical Engineering, University of Virginia, Charlottesville, VA, USA

[2] Department of Radiology, University of Virginia, Charlottesville, VA, USA

[3] Department of Electrical and Computer Engineering, University of Virginia, Charlottesville, VA, USA

Abstract

Newly-isolated serotypes of AAV readily cross the endothelial barrier to provide efficient transgene delivery throughout the body. However, tissue-specific expression is preferred in most experimental studies and gene therapy protocols. Previous efforts to restrict gene expression to the myocardium often relied on direct injection into heart muscle or intracoronary perfusion. Here, we report an AAV vector system employing the cardiac troponin T promoter (cTnT). Using luciferase and eGFP, the efficiency and specificity of cardiac reporter gene expression using AAV serotype capsids: AAV-1, 2, 6, 8 or 9 were tested after systemic administration to 1 week old mice. Luciferase assays showed that the cTnT promoter worked in combination with each of the AAV serotype capsids to provide cardiomyocyte-specific gene expression, but AAV-9 followed closely by AAV-8 was the most efficient. AAV9-mediated gene expression from the cTnT promoter was 640-fold greater in the heart compared to the next highest tissue (liver). eGFP fluorescence indicated a transduction efficiency of 96% using AAV-9 at a dose of only 3.15×10^{10} viral particles per mouse. Moreover, the intensity of cardiomyocyte eGFP fluorescence measured on a cell-by-cell basis revealed that AAV-mediated gene expression in the heart can be modeled as a Poisson distribution; requiring an average of nearly two vector genomes per cell to attain an 85% transduction efficiency.

Keywords

AAV; Cardiomyocyte-specific; Cardiac Troponin-T Promoter; Gene Therapy; Poisson distribution

Correspondence: Brent A. French, Ph.D., Department of Biomedical Engineering, 415 Lane Road, MR5 Building, Room 1219, University of Virginia, Charlottesville, VA 22903, Phone: (434) 924-5728, Fax: (434) 924-5923, bf4g@virginia.edu.

Conflict of Interest

The authors declare no conflict of interest.

Introduction

Important goals of contemporary biomedical research include elucidating the molecular basis of cardiovascular diseases and developing novel approaches for treatment and prevention. The development of efficient techniques for direct in vivo gene transfer is important not only to expedite basic science studies in animal models, but also to realize the considerable potential for direct clinical application. However, progress to date in human gene therapy has been limited by shortcomings in the available gene delivery systems. An ideal vector system for cardiac gene therapy would deliver genes efficiently and specifically to cardiomyocytes, provide for long term gene expression, would be free of immune responses, pose minimal risk to the host, and could be administered to the heart without complicated surgical procedures. In the past, a number of methods have been employed to focus viral-mediated gene delivery to the heart: primarily by direct injection into heart muscle[1, 2] and by complex intracoronary perfusion techniques requiring open-chest surgery to cross-clamp the aorta.[3, 4] The use of vascular permeabilizing agents such as histamine, papaverine or substance P with cardioplegia solution and/or whole body cooling have also been employed in attempts to improve the efficiency of conventional AAV-2 vectors for transducing skeletal and cardiac myocytes in vivo.[4, 5] Ironically, the conventional AAV serotype (AAV-2) used in the vast majority of the AAV studies performed to date suffers from a relatively low transduction rate and a prolonged lag phase (up to 6 weeks) before full expression is achieved in the heart.[6, 7] Despite these limitations, AAV-2 vectors have often favored for clinical gene therapy protocols due to their wide range of tissue tropism and minimal vector-related immunological complications (reviewed by Wu et al.).[8] More recently, a number of new AAV serotypes have been isolated, and some of these (e.g., AAV-1, AAV-6, AAV-8 and AAV-9) effectively cross the endothelial barrier to efficiently transduce a variety of organs.[9–13] The AAV-9 capsid has previously been reported to show a modest preference for cardiac tissue in vivo, both in one day old neonatal mice[10, 11] and in adult mice.[9] Moreover, it has been shown that AAV9 transduction to heart, lung and tibialis anterior muscle is superior and age-independent, whereas liver and kidney are transduced poorly in one day old neonates as compared to adult mice.[11]

The new AAV serotypes provide for early-onset transgene expression[9, 14] and mediate highly-efficient gene transfer to a variety of tissues in neonatal mice,[10, 11, 13] adult mice,[9–12] rats,[15] canines[16] and even non-human primates.[17] While desirable from the standpoint of general utility, the wide range of tissue tropism displayed by most AAV serotypes can become a liability in specific gene therapy applications where it is often important to restrict gene expression to a particular cell type. The incorporation of gene regulatory elements conferring tissue-specific gene expression has therefore been developed as general strategy for targeting gene therapy to particular tissues of interest.

As one of the 3 subunits of the troponin (troponin C, troponin T and troponin I) found in cardiac thin filaments, cardiac troponin T (cTnT) binds to tropomyosin to form the troponin-tropomyosin complex which plays an important role in regulating contractile function.[18] Ma et al., performed mutational analyses on the cTnT promoter region, and reported that the −375 to +43 region (relative to the cTnT transcriptional start site) is sufficient to confer cardiomyocyte-specific gene expression.[19] It follows that this truncated cTnT promoter

might prove useful for preferentially restricting therapeutic gene expression to cardiomyocytes in the heart, both for basic science experiments and for cardiac gene therapy protocols.

In the present study, we constructed AAV vectors in which the truncated cTnT promoter drives the expression of luciferase or eGFP. The resulting AAV vectors were packaged into a panel of AAV serotypes (AAV-1, 2, 6, 8 or 9). The minimal cTnT promoter sufficed to preferentially restrict gene expression almost exclusively to cardiomyocytes, even after systemic administration. We then administered AAV vectors expressing luciferase systemically, and compared the transduction efficiency of available AAV capsid serotypes. These experiments showed that AAV-9, closely followed by AAV-8, was the most efficient capsid serotype for cardiomyocyte gene delivery. Finally, we characterized the distribution of eGFP expression in the murine heart following AAV-9 mediated gene delivery via systemic injection and discovered that cellular fluorescence intensity follows a Poisson distribution, thus serving as a sensitive measure of the number of AAV genomes expressed in each cardiomyocyte at the cellular level. This finding, in turn, revealed that an average of two viral genomes per cell need to be expressed in order to assure that 85% of the cells express at least one genome (as predicted by Poisson distribution).

Results

The cTnT promoter directs cardiomyocyte-specific gene expression

An initial comparison of the AAV vectors harboring CMV and cTnT promoters (Fig 1A) was made using the most efficient capsid serotype available at the time (AAV-6). ACMVLuc or AcTnTLuc packaged in AAV-6 capsids were administered to one week-old mice by IV injection. In-vivo bioluminescence imaging revealed that luciferase expression was evident within three days after vector administration. Luciferase expression was observed throughout the entire body in mice injected with the ACMVLuc (Fig. 1B, CMV). However, in mice injected with the AcTnTLuc, expression was restricted to the left side of the thoracic cavity (Fig. 1B, cTnT). Ex-vivo bioluminescence imaging (Fig. 1C) on the various organs from these mice showed that, in ACMVLuc mice, luciferase expression was abundant in muscle tissues (heart, intercostal and gastrocnemius muscles) and liver (Fig. 1C, CMV). However, in mice that received AcTnTLuc, luciferease expression was predominantly found in the heart (Fig. 1C, cTnT). A quantitative analysis of luciferase expression was made by performing in vitro luciferase assays on the various organs as shown in Fig. 1D. In mice that received ACMVLuc, expression was mainly found in the muscle tissues and liver and to a lesser extent in kidney, lung, spleen and thymus. In intercostal muscle, expression from the CMV promoter was 9-fold higher than in the heart. However, in mice that received AcTnTLuc, luciferase expression was nearly 100-fold greater in the heart than in any other tissue assayed (including liver, intercostal and gastrocnemius muscle, Fig. 1D). These data clearly demonstrate that AAV-mediated gene expression from a truncated cTnT promoter is preferentially restricted to the heart following systemic administration.

AAV serotypes AAV-8 and AAV-9 provide superior transduction efficiency

After establishing the utility of the truncated cTnT promoter to preferentially restrict gene expression to the heart, a study was performed to compare the efficiency and specificity of cTnT-mediated cardiac gene expression using capsids from AAV serotypes 1, 2, 6, 8 and 9. Bioluminescence imaging of mice showed that luciferase signals were limited to the left side of the thoracic cavity in all mice irrespective of the serotype used (Fig. 2A). The light output was highest in mice that received reporter genes packaged in AAV-8 and AAV-9 capsids. Light output was significantly lower in mice that were injected with AAV-1 and AAV-6 capsids. Nevertheless, the AAV-1 and AAV-6 capsids were still far more efficient than conventional AAV-2, which produced very low levels of bioluminescence. In vitro luciferase assays performed on organ protein extracts from the same mice (Fig. 2B) confirmed that luciferase activity was lowest in the AAV-2 group. In comparison to the conventional AAV-2 capsid, cardiac luciferase expression was 26-fold higher with AAV-1, 28-fold higher with AAV-6, 271-fold higher with AAV-8 and 358-fold higher with AAV-9 capsids. These data show that serotype AAV-9 (followed closely by AAV-8) is far more efficient than serotypes AAV-2, AAV-1 and AAV-6 at delivering genes to the heart after IV injection. When delivered with the AAV-9 capsid, the cardiomyocyte-specific cTnT promoter directed levels of luciferase expression that were >640-fold higher in the heart than in the next highest tissues (liver, intercostal and gastrocnemius muscles).

AAV vectors provide homogeneous transduction to cardiomyocytes throughout the ventricular myocardium

In order to examine tissue distribution, the AAV vector AcTnTeGFP was packaged into capsids from AAV serotypes 1, 2, 6, 8 and 9. AAV vectors were administered to one week-old mice via jugular vein at doses of 3.15×10^{9}, 1×10^{10}, 3.15×10^{10} and 1×10^{11} viral genomes (vg) per mouse. In a one week-old 2.5 g mouse, these doses correspond to 1.26×10^{12}, 4×10^{12}, 1.26×10^{13} and 4×10^{13} vg/kg body weight, respectively. Four weeks following vector administration, 6 μm cryosections were prepared and analysis of eGFP expression by fluorescence microscopy revealed that AAV-2 transduced cardiomyocytes poorly even at the highest dose (1×10^{11} vg) tested (Figs. 3 and 4A). In contrast, AAV-9 transduced cardiomyocytes more efficiently than any other serotype tested. A transduction rate of 96±2% was observed with AAV-9 at a dose of only 3.15×10^{10} vg per mouse (Fig. 3 and 4A). With AAV-8, a 95±3% transduction rate was observed at the dose of 1×10^{11} vg/mouse. The superior transduction efficiency of AAV-9 over AAV-8 was even more evident at lower dose ranges (1×10^{10} vg/mouse and lower). With AAV-1 and 6, transduction efficiency was approximately 75% at the highest dose tested (1×10^{11} vg/mouse). Comparison of transduction efficiencies between the various serotypes at the dose of 3.15×10^{9} vg/mouse indicated that AAV-9 transduced cardiomyocytes 5.8-fold more efficiently than AAV-8 and 22-fold more efficiently than AAV-1 or -6.

AAV vectors deliver multiple genome copies per cell after systemic administration

Next, we determined the number of vector genome copies per cell as an independent measure of gene transfer efficiency for each of the AAV capsid serotypes. Four weeks following systemic vector administration, total genomic DNA was prepared from mouse

hearts, and mean vector genome copy numbers per μg of genomic DNA were determined by quantitative real-time PCR. The results are summarized in Fig. 4B. Mean vector copy numbers per cell increased linearly in a dose-dependent fashion for AAV serotypes -1, -6, -8, and −9 over doses ranging from 3.15×10^9 to 1×10^{11} vg/mouse (Fig. 4B). However, the vector copy numbers per cell transduced by AAV-2 increased by only 60% over this same dose range, indicating that AAV2 is poorly suited for cardiac gene delivery. Vector genome copy numbers per μg genomic DNA of $\sim 1 \times 10^6$ or higher were detected at the doses of 3.15×10^{10} for AAV-1 and AAV-6, 1×10^{10} for AAV-8 and 3.15×10^9 vg/mouse for AAV-9. These results confirm that serotype AAV-9 provides superior direct gene transfer in mouse hearts following systemic administration. The limitation of using "transduction efficiency" (as determined by counting transgene-positive cells) to quantitate direct gene transfer is illustrated in Fig. 4C, where the percentage of transduced cells (containing at least one vector genome) plateaus at 100% while the mean vector copy number per μg of genomic DNA continues to increase with increasing dose (Fig. 4B).

The specificity of the AAV9 capsid in combination with the cTnT promoter is evidenced by lack of eGFP expression in smooth muscle or endothelial cells within the heart

Low magnification fluorescence imaging of eGFP expression in mouse heart sections treated with the AcTnTeGFP vector packaged into AAV-9 capsids illustrates the homogeneous distribution of gene expression seen throughout the right and left ventricles of the heart (Fig. 5A). Fluorescence imaging at medium magnification (Fig. 5B) shows the position of arteriole (indicated by box) that is shown under high magnification in Fig. 5C. Close examination of this image reveals that the smooth muscle and endothelial cells are completely devoid of fluorescence, even while the internal elastic lamina exhibits the anticipated autofluorescence and cardiomyocytes surrounding the arterioles were intensely positive for eGFP expression. Immunohistochemical analyses performed on serial sections confirmed eGFP expression exclusively in cardiomyocytes, and not in vascular smooth muscle or endothelial cells (Supplementary Fig. S1). This result further emphasizes the specificity with which the combination of the AAV9 capsid and the cTnT promoter preferentially restrict gene expression to cardiomyocytes within the heart.

eGFP fluorescence reveals that direct gene transfer follows a Poisson distribution

Careful scrutiny of eGFP fluorescence images (Figs. 3, 5A-D and 6A) revealed that the intensity of eGFP fluorescence in individual cardiomyocytes appeared to reflect a gene-dose effect. That is, the variation in eGFP fluorescence intensity between cells did not appear to be random, but rather exhibited a quantal property, such that eGFP-positive cells could be clustered into groups of cells that exhibited similar levels of fluorescence intensity (see Fig. 6A). To pursue this observation, quantitative image analysis was performed on heart cryosections from mice transduced with AcTnTeGFP packaged in AAV8 and AAV-9 at intermediate doses (3.15×10^9 and 1×10^{10} vg/mouse). K-means cluster analysis of cardiomyocyte fluorescence intensities indeed confirmed that these intensities clustered around integer values, and one-way ANOVA followed by Dunnett's T3 post-hoc analysis confirmed that each cluster was significantly different from any other ($p<0.05$ for any pairwise comparison). Figure 6 illustrates an example of this analysis, performed on a mouse injected with AAV-9 at a dose of 1×10^{10} vg/mouse. The histogram resulting from cluster

analysis of cardiomyocyte intensities shown in Fig. 6A is shown in Fig. 6B, where the colors red, green, blue, light blue, purple and yellow were used to represent n = 0, 1, 2, 3, 4 and ≥ 5 AAV genomes per cell, respectively. Each cardiomyocyte in Fig. 6A was then retrospectively color-coded according to the same classification scheme for illustrative purposes as shown in Fig. 6C. The percentage of cardiomyocytes in each cluster (Fig. 6D, Actual) was then used to compute the overall mean number of viral genomes per cell over all clusters (n = 2.0) and this mean was used as the Poisson parameter ($\lambda = 2.0$) to generate the theoretical Poisson distribution (Fig. 6D, Poisson Mean = 2.0). Finally, the analysis was repeated with AAV-9 at another dose (3.15×10^9 vg/mouse), and again with AAV-8 at two doses (3.15×10^9 and 1×10^{10} vg/mouse, see Supplemental Figures S1–S3). Together, the results of image analysis yielded a set of 24 actual values for the percentages of cells in each FOV containing n = 0, 1, 2, 3, 4 or ≥ 5 expressed viral genomes per cell (6 of which are illustrated in Fig. 6D). The actual values were then correlated with the theoretical values obtained from the corresponding Poisson distributions in Fig. 6E to illustrate the predictive power of this approach. The strong correlation ($R^2 = 0.85$) suggests a linkage between the intensity of eGFP fluorescence and vector genome copy number per cell, and that the intensity of eGFP fluorescence on a per cardiomyocyte basis can be modeled in terms of a Poisson distribution.

Discussion

The newly-isolated AAV serotypes (AAV-1, -6, -8 and -9) have been shown to deliver genes efficiently to various organs including skeletal muscle, heart, liver and lung, and to provide sustained gene expression following systemic administration[9, 10, 12, 13, 20]. The wide range of tissue tropism exhibited by the various AAV serotypes indicates that AAV should have broad utility in delivering genes to multiple organ systems, but the treatment of individual diseases often calls for restricting therapeutic gene expression to a particular target organ or cell type. Therapeutic genes placed under the control of strong viral promoters produce high levels of protein expression with minimal tissue specificity (e.g., Fig. 1B, CMV). However, the expression of therapeutic genes in off-target tissues can often lead to deleterious side effects. Local delivery to the heart via intramuscular injection may be possible in a subset of cardiac procedures such as coronary artery bypass graft (CABG) surgery or during interventional procedures which might include catheter-based injection into the myocardium.[21] However, these approaches are not only invasive, they require high-density injection matrices in order to achieve homogeneous patterns of gene expression. The present study investigated the utility of combining a cardiomyocyte-specific promoter with capsids from the recently isolated AAV serotypes (AAV-1, -6, -8 and -9) to achieve stable, cardiomyocyte-specific gene expression following IV administration in mice.

Recombinant AAV genomes of up to 5.2 kb in length can be packaged into AAV capsids without compromising infectivity. Due to this packaging constraint, it is desirable to minimize promoter size in order to accommodate larger therapeutic payloads. Previously, Aikawa et al. reported cardiomyocyte-specific gene expression from an AAV vector harboring a 363 base pair (−344 to +19) alpha myosin heavy chain promoter (α-MHC) packaged in AAV-2 capsids after direct injection into myocardial wall, liver, skeletal muscle and brain.[6] While the α-MHC promoter would appear to be similar in size, strength and

specificity to the cTnT promoter used here, the limited efficiency of the AAV-2 capsid made direct intramyocardial injection necessary in the previous study, whereas the high efficiency and natural cardiotropism of the AAV9 capsid supported IV administration in the current study. Su et al. used an AAV-2 vector carrying the MLC-2v promoter in combination with hypoxia response elements for ischemic heart specific gene expression after direct injection into myocardium.[22] More recently, Muller et al. used a 1.5 kb MLC promoter in combination with CMV enhancer elements and tested the efficiency of cardiac-specific gene expression from AAV serotypes AAV-1, AAV-2, AAV-4, AAV-5, AAV-6 and the mutant AAV-2 (R484E, R585E). The most efficient serotype was AAV-6, with mutant AAV-2 providing cardiac-specific gene expression in Sprague-Dawley rats following systemic administration.[23] Raake et al., constructed an AAV vector harboring a 1.5 kb hybrid promoter, composed of the CMV enhancer fused with rat myosin light chain promoter (CMV-MLC2v), packaged into AAV-2 or AAV-6 and demonstrated cardiomyocyte-specific gene expression following vector administration by pressure-regulated retro-infusion of the anterior interventricular cardiac vein.[24] However, the 1.5 kb CMV-MLC2v fusion promoter occupies 29% of the cloning space in AAV vector, leaving only 3.4 kb for inserting the gene of interest and polyadenylation signals. In contrast, the cTnT promoter reported here occupies <10% of the cloning space in AAV and provides robust, cardiomyocyte-specific expression even after systemic injection. While the minimal cTnT promoter employed here is only 411 bp[19] in length, it nevertheless confers a high degree of cardiomyocyte specificity without an appreciable loss in promoter strength relative to the ubiquitously active and strong CMV promoter (Fig. 1B). Using the cTnT promoter packaged in AAV9 capsids, the level of luciferase expression was >640-fold higher in the heart than in the next most highly expressing tissue (liver, followed closely by intercostal and gastrocnemius muscles). This remarkable degree of specificity was achieved while retaining >40% of the strength available from the CMV promoter. Irrespective of the AAV serotype that was tested, the cTnT promoter preferentially restricted gene expression to heart (Fig. 2). In order to confirm these findings, immunohistochemistry for eGFP and α-smooth muscle actin was performed on serial heart tissue sections from a mouse previously treated with the AAV-9 vector expressing eGFP from the cTnT promoter. The results indicated that eGFP expression was abundant in cardiomyocytes, but was virtually undetectable in vascular smooth muscle or endothelial cells (Supplementary Fig. S1).

The luciferase results in Fig. 2 indicate that AAV-9 transduces the heart 1.3 and 14-fold more efficiently than AAV-8 or AAV-1, respectively. The superior transduction of cardiomyocytes by serotype AAV-9 over AAV-8 after IV administration in mice is consistent with two previous reports.[9], [10] However, direct comparisons to these previous studies are not possible since they used a different reporter system (beta-galactosidase) and assays were performed at different time points after IV injection (2 weeks[9] and 4 weeks[10]). These distinctions notwithstanding, multiple groups using a variety of promoters, reporter systems and times to follow-up have consistently found that the AAV-9 capsid is more efficient for cardiac gene transfer than any other capsid tested to date. While all injections reported here were performed in one week-old mice, this strategy was employed only to take advantage of their low body weight in minimizing the amount of vector needed for each experiment. In recent studies, we found that the same weight-adjusted dose (vg per gram

body weight) yielded similar levels of gene expression in adult mice as when injected in week-old mice (data not shown). Furthermore, the time course of cardiac gene expression from the cTnT promoter after AAV9-mediated gene transfer in adult mice is consistent with the time course previously published for the non-tissue-specific CB promoter.[25]

In human gene therapy protocols, viral vector burden should be kept to the minimum to avoid vector-related side effects. It is therefore critical to determine the minimal gene dose necessary to achieve therapeutic effect. In the case of a secreted gene product, it may not be necessary to transduce every cell in the target organ. But for most therapeutic genes that remain intracellular, it will be desirable to obtain a uniform distribution of gene expression with transduction efficiencies approaching 100%. From this perspective, the results summarized in Fig. 6 are particularly enlightening because they reveal that AAV-mediated gene delivery follows a Poisson distribution.

The Poisson distribution provides a model for the number of discrete events occurring in a specified space or time interval. It is assumed that the events are independent of one another, and that the expected number of such events can be specified over a significant space/time interval. A well-studied example of a spatial Poisson process is the number of raindrops falling on a detector (i.e., a disdrometer).[26] In this case, the process of counting raindrops within a specified area has no memory in the sense that one raindrop falling does not affect another. By analogy, we show here (for the first time) that the same law may govern the number of AAV particles transducing individual cardiomyocytes during direct in vivo gene transfer.

It has previously been shown that the majority of the AAV genomes in muscle cells persist as transcriptionally active monomeric or head-to tail circular concatemeric episomes.[27], [28] Thus the level of gene expression resulting from AAV-mediated gene delivery to cardiomyocytes (and perhaps other muscle cells) should primarily be determined by gene dose and may be independent of genomic mechanisms such as gene silencing, chromosomal localization and histone modification. It has previously been proposed that viral-mediated gene transfer might follow a Poisson distribution in vitro,[29] but no supporting evidence was provided. In contrast, the close correlation between our empirical results and the theoretical results predicted by the Poisson distribution (Fig. 6E) suggests that the level of transgene expression in an AAV-transduced cardiomyocyte is primarily a function of gene-dose, and establishes a method for determining gene-dose on a cell-by-cell basis by performing image analysis on histological sections. The image analysis in the current study was motivated by the hypothesis that doubling (or tripling, quadrupling, etc.) the number of reporter genes per cell would follow the same general law of gene dose illustrated by haploid insufficiency. That is, transcription and translation are seldom rate-limiting, and doubling the number of genes in a cell will often double the amount of protein produced.

When considered in light of Poisson, Fig. 6D illustrates that it will be necessary (for example) to introduce an average of nearly two AAV genomes per cell in order to assure that 85% of target cells express at least one gene. This highlights the fact that direct gene transfer is fundamentally different from transgenesis or homologous recombination, because germ-line transmission of only a single gene is sufficient to insure its delivery to 100% of

the cells in a tissue; whereas for direct gene transfer, a mean hit-rate of one vector genome per cell is only adequate to insure that 63% of the cells will express at least one genome, and a mean of 5 vector genomes per cell is necessary to target >99% of the cells in a tissue (as defined by the Poisson distribution, see Fig. S4, Panel E in Supplementary Information).

These results also have important ramifications for the interpretation of eGFP expression in studies of direct in vivo gene transfer. That is, eGFP has not always been preferred as a reporter gene for studies of gene transfer to the heart, in part because it can be difficult to distinguish authentic eGFP fluorescence above endogenous background autofluorescence unless the promoter is quite strong. Nevertheless, several previous studies have used eGFP as a reporter gene to monitor AAV-mediated direct gene transfer to the heart.[30], [31] Interestingly, at least two of these studies used the ubiquitously strong CMV promoter, and the same quantal pattern of fluorescence intensity reported here is indeed evident in the previous fluorescence photomicrographs of eGFP expression.[30], [31] While the quantal pattern of authentic eGFP expression is clear in these figures, this pattern has not previously been explained, perhaps because the method of direct intra-myocardial injection[31] or lower transduction rates[30] made the quantal pattern less striking (compare for example, the top and bottom rows in Fig. 3).

While this report identifies a new approach for the quantitative determination of vector genomes per cell via image analysis of biofluorescence intensities in tissue sections, the limitations should also be acknowledged. This approach is not applicable unless the promoter is strong enough to produce enough fluorescent protein to be detected above endogenous autofluorescence. Furthermore, it is difficult to apply this technique when the mean hit-rate exceeds between 5–10 vector genomes per cell, because this may exceed the linear range that can be accommodated by a single exposure, causing cluster analysis to fail (see bottom right panel in Fig. 3). Thus the dynamic range of this approach is currently limited to mean hit-rates between 0.1 to 10 vector genomes per cell. Fortunately, this corresponds to a physiologically significant range: i.e., transduction efficiencies (as defined by >1 vector genome per cell) of 10 to 100%. Finally, this approach depends upon efficient, homogeneous methods of vector delivery (intra-venous or intra-arterial) and cannot be applied until after gene expression has reached an equilibrium state in non-dividing cells.

The >600-fold level of tissue-specificity obtained here by employing the cTnT promoter in combination with the highly-efficient AAV9 capsid should immediately prove useful in expediting small animal studies of cardiac gene function, both in normal and diseased states. However, it should be acknowledged that the tissue tropisms displayed by the various AAV serotypes have been shown to vary between species.[16] Furthermore, transcriptional targeting with tissue-restricted promoters does not reduce gene transfer to off-target tissues, only the levels of off-target gene expression. It should be possible to reduce viral burden, and further improve the safety profile of the highly-efficient AAV serotypes for cardiac gene therapy, by targeting transduction more specifically to cardiomyocytes. The potential of genetically engineering the AAV capsid to achieve transductional targeting to the heart has already been demonstrated in the context of AAV2,[23] albeit at significantly lower transduction efficiencies than possible with AAV9. Thus the strategy of combining transcriptional and transductional targeting[23], [32] with highly-efficient AAV serotypes holds significant promise

for the future of both basic science and translational research applications in the cardiovascular system.

Materials and Methods

Plasmids

The AAV vectors used in this study were derived from pACS: an AAV vector-generating plasmid composed of the 588 bp CMV IE promoter (from pCEP4, Invitrogen Corp, Carlsbad, CA), a multiple cloning site and an SV40 poly-adenylation signal flanked by AAV-2 ITRs.[33] To create an AAV vector-generating plasmid in which the CMV IE promoter drives the expression of the firefly luciferase gene (pCMVLuc), a 2.2 kb HindIII-BamHI fragment carrying the firefly luciferase cDNA was excised from plasmid pGL3 (Promega, Madison, WI, USA) and inserted between the HindIII and BamHI sites of pACS[33] (Fig. 1A). Plasmid pAcTnT is an AAV-generating plasmid harboring a truncated 418 bp chicken cTnT promoter (spanning from 375 nucleotides upstream to 43 nucleotides downstream of the cTnT transcriptional start site), a multiple cloning site and an SV40 polyadenylation signal. The cTnT promoter was PCR amplified using forward primer 5′-GCTCAGTCTAGAGCAGTCTGGGCTTTCACAAGAC-3′ and reverse primer 5′-GCTCAGAAGCTTAGGTCCCACGGAGCGGT-3′ containing XbaI and HindIII restriction sites, respectively. Plasmid AcTnT was derived from plasmid pACS in two steps. First, a 0.8 kb CMV promoter was excised from plasmid pACS with XbaI and HindIII digestion, and then the PCR-amplified cTnT promoter was inserted between the same restriction sites. To construct AcTnTLuc (Fig. 1A), the 2.2 kb firefly luciferase cDNA from plasmid pGL3 was excised as a HindIII-BamHI fragment and inserted between the HindIII and BamHI sites of pAcTnT. To construct AcTnTeGFP, an ~800 bp HindIII-NotI fragment encoding eGFP from pEGFP-N1 (Clontech, Palo Alto, CA, USA) was inserted between the HindIII and NotI sites of pAcTnT.

AAV vector production and purification

AAV vectors were packaged by the double or triple transfection method in HEK 293 cells.[34] AAV vectors were packaged into capsids from AAV-2, AAV-1 and AAV-6 using helper plasmids pSH5 [35] (gift from Dr. James Trempe), pDP1 and pDP6[36] (gifts from Dr. Mark Kay), respectively, using the double transfection method. AAV vectors were packaged into AAV-8 and AAV-9 capsids by the triple transfection method using helper plasmids pAdΔF6 (providing the three adenoviral helper genes) and plasmids p5E18-VD2/8 or p5E18-VD2/9[37], [38] (kindly provided by Dr. James M. Wilson). The AAV-generating plasmids and helper plasmid(s) were transfected into HEK 293 cells by the calcium-phosphate co-precipitation method.[39] Fifty μg of plasmid DNA (mixed in equimolar ratio) was used per 15 cm cell culture plate. Three days following transfection, AAV vectors were purified by ammonium sulfate fractionation and iodixanol gradient centrifugation.[40] Virus particles were resuspended in 1 ml of DPBS-MK, dialyzed against DPBS-MK and stored at −80°C.

Determination of AAV vector titer

Titers for the AAV vectors (viral genomes/ml) were determined by quantitative real-time PCR as described previously.[7] The following primers were used for amplifying luciferase:

5′-AGAACTGCCTGCGTGAGATT-3′ (forward) and 5′-AAAACCGTGATGGAATGGAA-3′ (reverse), and eGFP: 5′-CACATGAAGCAGCACGACTT-3′ (forward) and 5′-GAAGTTCACCTTGATGCCGT-3′ (reverse). Known copy numbers (10^5–10^8) of the respective plasmids (pAcTnTLuc or pAcTnTeGFP) carrying the appropriate cDNAs were used to construct standard curves.

Animal procedures

All work was performed under animal protocols approved by the Institutional Animal Care and Use Committee and conformed to the "Guide for the Care and Use of Laboratory Animals" (NIH Publication 85-23, revised 1985). C57BL/6 breeding pairs were purchased from The Jackson Laboratories (Bar Harbor, ME) and maintained on a 12/12 hr light/dark cycle at 24°C and 60% humidity. All direct gene transfer was carried out using one-week-old C57BL/6 mice weighing 2.0–2.5 g. For IV injection, mice were anesthetized with 1–1.2% isoflurane in oxygen while ~20 μl of viral solution was slowly injected via jugular vein.

Bioluminescence imaging

Luciferase activity in mouse hearts was non-invasively assessed by in vivo bioluminescence imaging using previously reported methods.[7, 41] Ex vivo bioluminescence imaging of isolated tissues (heart, liver, thymus, kidney, spleen, brain, gastrocnemius and intercostal muscle) was performed as described previously.[7] All bioluminescence imaging was performed using an IVIS 100 system (Caliper Life Sciences, Hopkinton, MA).

In vitro luciferase assay

In vitro luciferase assays were performed using luciferase assay reagents from Promega Corp. (Madison, WI). Heart, liver, thymus, kidney, spleen, brain, gastrocnemius and intercostal muscle were collected from mice after bioluminescence imaging and euthanasia at 4 weeks post-injection. Protein extracts were prepared from whole organs as recommended by the manufacturer. Relative light units (RLU) of luciferase activity were determined using a FLUOstar Optima micro-plate reader (BMG Labtech, Durham, NC).

Fluorescence imaging and immunohistochemistry

eGFP expression in the mouse heart was documented by fluorescence imaging and immunohistochemical analysis. Four weeks following vector administration, animals were euthanized and hearts were collected and fixed in 3.7% para-formaldehyde for 1 h at 4°C. After washing in PBS (3 times, 5 min each), hearts were equilibrated with 30% sucrose in PBS overnight. Six μm cryosections were prepared and eGFP expression was documented using a BX51 fluorescence microscope with a DP70 digital camera (Olympus America, Inc., Center Valley, PA). To determine transduction efficiency, a minimum of 3 fields at 20x magnification were captured from the mid-ventricular sections of 2–3 hearts for each group. The percentage of the total tissue area showing eGFP expression was calculated using Adobe Photoshop (Adobe Systems Inc. San Jose CA). In some cases, the same sections used for fluorescence imaging were subsequently immunostained for eGFP using a rabbit anti-GFP antibody (Abcam Inc, Cambridge, MA).

Determination of AAV vector genome copy number per μg genomic DNA

The AAV vector AcTnTeGFP was packaged into capsids from AAV serotypes 1, 2, 6, 8 and 9. AAV vectors were administered at doses ranging from 3.15×10^{9} to 1×10^{11} viral genomes (vg) via jugular vein in one week-old mice. Four weeks following vector administration, total genomic DNA from the mouse hearts was prepared by standard phenol-chloroform extraction. Real-time quantitative PCR using SYBR Green I detection was performed on a BioRad iCycler using 100ng samples of genomic DNA. The following primers were used for amplifying eGFP: 5′-CACATGAAGCAGCACGACTT-3′ (forward) and 5′-GAAGTTCACCTTGATGCCGT-3′ (reverse). Known copy numbers (10^{3}–10^{8}) of the plasmid pAcTnTeGFP were used to construct the standard curve. The results were expressed as mean AAV vector genome copy numbers/μg of genomic DNA.

Image analysis of heart cryosections for quantification of AAV vector genome copies/cell

In order to test the hypothesis that fluorescence intensity was related to the number of AAV vector genomes per cell, eGFP fluorescence intensities from individual cardiomyocytes within representative fields of view in heart cryosections were measured and subject to image analysis. Thus representative fields of view (FOV) were converted to 8-bit gray scale so that the image intensities of individual cardiomyocytes could be sampled using Photoshop (Adobe Systems Inc. San Jose CA). Towards this end, a consistently-sized region of interest within each cardiomyocyte was chosen that avoided both the nucleus and cell membrane, and the mean intensity of that region was recorded along with the location of the sampled cardiomyocyte. A k-means clustering algorithm was then applied to the intensity values for every cardiomyocyte within the FOV, yielding six clusters of image intensity. K-means clustering is a method that seeks to partition “n” observations into “k” clusters, so that each observation is assigned to the cluster with the nearest mean.[42] The percentage of cardiomyocytes in each cluster was then used to compute the overall mean number of viral genomes per cell over all clusters and this mean was used as the Poisson parameter (λ) to generate the theoretical Poisson distribution. Finally, the actual percentages of cardiomyocytes in each cluster (as determined by image analysis) were correlated with the theoretical percentage values determined from the corresponding Poisson distributions.

Statistics

Data are reported as mean +/− standard error. K-means cluster analysis was applied to image intensity values to test the hypothesis that these values represented distinct groups. The hypothesis that each of the resulting groups were different was tested by one-way ANOVA, followed by Dunnett’s T3 post-hoc test when variances were not equal between groups. All statistical analyses were performed with the SPSS Statistics package (SPSS Inc., Chicago, IL).

Supplementary Material

Refer to Web version on PubMed Central for supplementary material.

Acknowledgments

Funding sources: This work was supported by NIH R01s HL058582 and HL069494 (to BAF).

The authors wish to acknowledge Dr. James Trempe for pSH5, Dr. Mark Kay for pDP1 and pDP6, and Dr. James Wilson for p5E18-VD2/8 and p5E18-VD2/9. This work was supported by NIH R01s HL058582 and HL069494 (to BAF).

References

1. Su H, Lu R, Kan YW. Adeno-associated viral vector-mediated vascular endothelial growth factor gene transfer induces neovascular formation in ischemic heart. Proceedings of the National Academy of Sciences of the United States of America. 2000; 97(25):13801–6. [PubMed: 11095751]
2. Svensson EC, Marshall DJ, Woodard K, Lin H, Jiang F, Chu L, et al. Efficient and stable transduction of cardiomyocytes after intramyocardial injection or intracoronary perfusion with recombinant adeno-associated virus vectors. Circulation. 1999; 99(2):201–5. [PubMed: 9892583]
3. Champion HC, Georgakopoulos D, Haldar S, Wang L, Wang Y, Kass DA. Robust adenoviral and adeno-associated viral gene transfer to the in vivo murine heart: application to study of phospholamban physiology. Circulation. 2003; 108(22):2790–7. [PubMed: 14638552]
4. Iwatate M, Gu Y, Dieterle T, Iwanaga Y, Peterson KL, Hoshijima M, et al. In vivo high-efficiency transcoronary gene delivery and Cre-LoxP gene switching in the adult mouse heart. Gene Therapy. 2003; 10(21):1814–20. [PubMed: 12960971]
5. Greelish JP, Su LT, Lankford EB, Burkman JM, Chen H, Konig SK, et al. Stable restoration of the sarcoglycan complex in dystrophic muscle perfused with histamine and a recombinant adeno-associated viral vector. Nature Medicine. 1999; 5(4):439–43.
6. Aikawa R, Huggins GS, Snyder RO. Cardiomyocyte-specific gene expression following recombinant adeno-associated viral vector transduction. Journal of Biological Chemistry. 2002; 277(21):18979–85. [PubMed: 11889137]
7. Prasad K-MR, Xu Y, Yang Z, Toufektsian M-C, Berr SS, French BA. Topoisomerase inhibition accelerates gene expression after adeno-associated virus-mediated gene transfer to the mammalian heart. Molecular Therapy: the Journal of the American Society of Gene Therapy. 2007; 15(4):764–71. [PubMed: 17299410]
8. Wu Z, Asokan A, Samulski RJ. Adeno-associated virus serotypes: vector toolkit for human gene therapy. Molecular Therapy: the Journal of the American Society of Gene Therapy. 2006; 14(3): 316–27. [PubMed: 16824801]
9. Inagaki K, Fuess S, Storm TA, Gibson GA, McTiernan CF, Kay MA, et al. Robust systemic transduction with AAV9 vectors in mice: efficient global cardiac gene transfer superior to that of AAV8. Molecular Therapy: the Journal of the American Society of Gene Therapy. 2006; 14(1):45–53. [PubMed: 16713360]
10. Pacak CA, Mah CS, Thattaliyath BD, Conlon TJ, Lewis MA, Cloutier DE, et al. Recombinant adeno-associated virus serotype 9 leads to preferential cardiac transduction in vivo. Circulation Research. 2006; 99(4):e3–9. [PubMed: 16873720]
11. Bostick B, Ghosh A, Yue Y, Long C, Duan D. Systemic AAV-9 transduction in mice is influenced by animal age but not by the route of administration. Gene Therapy. 2007; 14 (22):1605–9. [PubMed: 17898796]
12. Gregorevic P, Blankinship MJ, Allen JM, Crawford RW, Meuse L, Miller DG, et al. Systemic delivery of genes to striated muscles using adeno-associated viral vectors. Nature Medicine. 2004; 10(8):828–34.
13. Wang Z, Zhu T, Qiao C, Zhou L, Wang B, Zhang J, et al. Adeno-associated virus serotype 8 efficiently delivers genes to muscle and heart. Nature Biotechnology. 2005; 23 (3):321–8.
14. Thomas CE, Storm TA, Huang Z, Kay MA. Rapid uncoating of vector genomes is the key to efficient liver transduction with pseudotyped adeno-associated virus vectors. Journal of Virology. 2004; 78(6):3110–22. [PubMed: 14990730]

15. Palomeque J, Chemaly ER, Colosi P, Wellman JA, Zhou S, Del Monte F, et al. Efficiency of eight different AAV serotypes in transducing rat myocardium in vivo. [erratum appears in Gene Ther. 2007 Jul;14(13):1055]. Gene Therapy. 2007; 14(13):989–97. [PubMed: 17251988]
16. Yue Y, Ghosh A, Long C, Bostick B, Smith BF, Kornegay JN, et al. A single intravenous injection of adeno-associated virus serotype-9 leads to whole body skeletal muscle transduction in dogs. Molecular Therapy: the Journal of the American Society of Gene Therapy. 2008; 16(12):1944–52. [PubMed: 18827804]
17. Gao G-P, Lu Y, Sun X, Johnston J, Calcedo R, Grant R, et al. High-Level Transgene Expression in Nonhuman Primate Liver with Novel Adeno-Associated Virus Serotypes Containing Self-Complementary Genomes. J Virol. 2006; 80(12):6192–6194. [PubMed: 16731960]
18. Marian AJ, Roberts R. The molecular genetic basis for hypertrophic cardiomyopathy. Journal of Molecular & Cellular Cardiology. 2001; 33(4):655–70. [PubMed: 11273720]
19. Ma H, Sumbilla CM, Farrance IKG, Klein MG, Inesi G. Cell-specific expression of SERCA, the exogenous Ca2+ transport ATPase, in cardiac myocytes. American Journal of Physiology - Cell Physiology. 2004; 286(3):C556–64. [PubMed: 14592812]
20. Nakai H, Fuess S, Storm TA, Muramatsu S-i, Nara Y, Kay MA. Unrestricted hepatocyte transduction with adeno-associated virus serotype 8 vectors in mice. Journal of Virology. 2005; 79(1):214–24. [PubMed: 15596817]
21. Kornowski R, Leon MB, Fuchs S, Vodovotz Y, Flynn MA, Gordon DA, et al. Electromagnetic guidance for catheter-based transendocardial injection: a platform for intramyocardial angiogenesis therapy. Results in normal and ischemic porcine models. Journal of the American College of Cardiology. 2000; 35(4):1031–9. [PubMed: 10732905]
22. Su H, Kan YW. Adeno-associated viral vector-delivered hypoxia-inducible gene expression in ischemic hearts. Methods in Molecular Biology. 2007; 366:331–42. [PubMed: 17568134]
23. Muller OJ, Leuchs B, Pleger ST, Grimm D, Franz W-M, Katus HA, et al. Improved cardiac gene transfer by transcriptional and transductional targeting of adeno-associated viral vectors. Cardiovascular Research. 2006; 70(1):70–8. [PubMed: 16448634]
24. Raake PW, Hinkel R, Muller S, Delker S, Kreuzpointner R, Kupatt C, et al. Cardio-specific long-term gene expression in a porcine model after selective pressure-regulated retroinfusion of adeno-associated viral (AAV) vectors. Gene Therapy. 2008; 15(1):12–7. [PubMed: 17943147]
25. Bish LT, Morine K, Sleeper MM, Sanmiguel J, Wu D, Gao G, et al. AAV9 Provides Global Cardiac Gene Transfer Superior to AAV1, AAV6, AAV7, and AAV8 in the Mouse and Rat. Human Gene Therapy. 2008 0(ja).
26. Uijlenhoet R, Stricker JNM, Torfs PJJF, Creutin JD. Towards a Stochastic Model of Rainfall for Radar Hydrology: Testing the Poisson Homogeneity Hypothesis. Physics and Chemistry of the Earth, Part B: Hydrology, Oceans and Atmosphere. 1999; 24:747–755.
27. Duan D, Sharma P, Yang J, Yue Y, Dudus L, Zhang Y, et al. Circular intermediates of recombinant adeno-associated virus have defined structural characteristics responsible for long-term episomal persistence in muscle tissue. [Erratum appears in J Virol 1999 Jan;73(1):861]. Journal of Virology. 1998; 72(11):8568–77. [PubMed: 9765395]
28. Schnepp BC, Clark KR, Klemanski DL, Pacak CA, Johnson PR. Genetic fate of recombinant adeno-associated virus vector genomes in muscle. Journal of Virology. 2003; 77 (6):3495–504. [PubMed: 12610125]
29. Fehse B, Kustikova OS, Bubenheim M, Baum C. Pois(s)on - It's a Question of Dose. Gene Ther. 2004; 11(11):879–881. [PubMed: 15057265]
30. Vassalli G, Büeler H, Dudler J, von Segesser LK, Kappenberger L. Adeno-associated virus (AAV) vectors achieve prolonged transgene expression in mouse myocardium and arteries in vivo: a comparative study with adenovirus vectors. International Journal of Cardiology. 2003; 90(2–3): 229–238. [PubMed: 12957756]
31. Du L, Kido M, Lee DV, Rabinowitz JE, Samulski RJ, Jamieson SW, et al. Differential Myocardial Gene Delivery by Recombinant Serotype-Specific Adeno-associated Viral Vectors. Mol Ther. 2004; 10(3):604–608. [PubMed: 15336660]

32. Barker SD, Dmitriev IP, Nettelbeck DM, Liu B, Rivera AA, Alvarez RD, et al. Combined transcriptional and transductional targeting improves the specificity and efficacy of adenoviral gene delivery to ovarian carcinoma. Gene Ther. 10(14):1198–1204. [PubMed: 12833129]

33. Prasad KM, Yang Z, Bleich D, Nadler JL. Adeno-associated virus vector mediated gene transfer to pancreatic beta cells. Gene Therapy. 2000; 7(18):1553–61. [PubMed: 11021593]

34. Xiao X, Li J, Samulski RJ. Production of high-titer recombinant adeno-associated virus vectors in the absence of helper adenovirus. Journal of Virology. 1998; 72(3):2224–32. [PubMed: 9499080]

35. Collaco RF, Cao X, Trempe JP. A helper virus-free packaging system for recombinant adeno-associated virus vectors. Gene. 1999; 238(2):397–405. [PubMed: 10570967]

36. Grimm D, Kay MA, Kleinschmidt JA. Helper virus-free, optically controllable, and two-plasmid-based production of adeno-associated virus vectors of serotypes 1 to 6. Molecular Therapy: the Journal of the American Society of Gene Therapy. 2003; 7(6):839–50. [PubMed: 12788658]

37. Gao G, Vandenberghe LH, Alvira MR, Lu Y, Calcedo R, Zhou X, et al. Clades of Adeno-associated viruses are widely disseminated in human tissues. Journal of Virology. 2004; 78 (12): 6381–8. [PubMed: 15163731]

38. Gao G-P, Alvira MR, Wang L, Calcedo R, Johnston J, Wilson JM. Novel adeno-associated viruses from rhesus monkeys as vectors for human gene therapy. Proceedings of the National Academy of Sciences of the United States of America. 2002; 99(18):11854–9. [PubMed: 12192090]

39. Jordan M, Schallhorn A, Wurm FM. Transfecting mammalian cells: optimization of critical parameters affecting calcium-phosphate precipitate formation. Nucleic Acids Research. 1996; 24(4):596–601. [PubMed: 8604299]

40. Ried MU, Girod A, Leike K, Buning H, Hallek M. Adeno-associated virus capsids displaying immunoglobulin-binding domains permit antibody-mediated vector retargeting to specific cell surface receptors. Journal of Virology. 2002; 76(9):4559–66. [PubMed: 11932421]

41. Wu JC, Inubushi M, Sundaresan G, Schelbert HR, Gambhir SS. Optical imaging of cardiac reporter gene expression in living rats. Circulation. 2002; 105(14):1631–4. [PubMed: 11940538]

42. Acton ST, Mukherjee DP. Scale space classification using area morphology. IEEE Transactions on Image Processing. 2000; 9(4):623–635. [PubMed: 18255435]

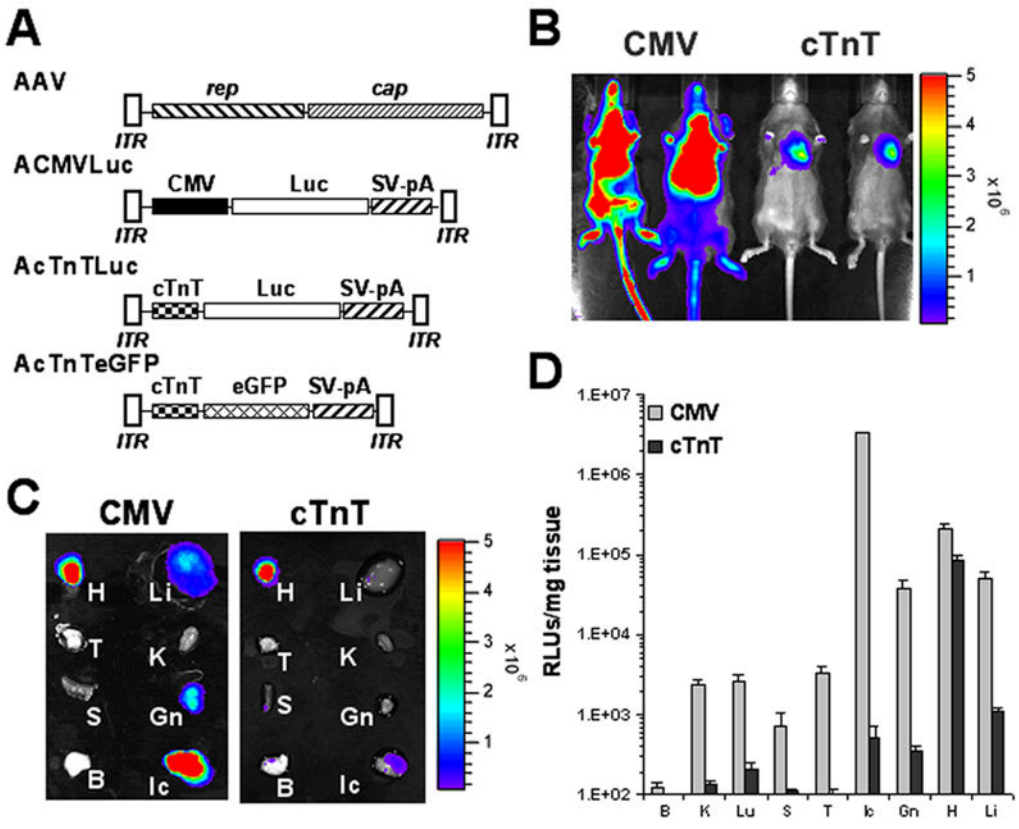

Fig. 1.

(A) Schematic representation of wild type AAV and AAV vectors: ACMVLuc and AcTnTLuc carry the firefly luciferase cDNA driven by CMV and cTnT promoters, respectively. AcTnTeGFP encodes eGFP protein driven by the cTnT promoter. AAV inverted terminal repeats (ITR), and SV40 poly-adenylation (pA) are also indicated. B, Bioluminescence imaging illustrates cardiomyocyte-specific gene expression directed by the cTnT promoter. The AAV vectors [ACMVLuc (CMV) and AcTnTLuc (cTnT)] were packaged into AAV-6 capsids. One week old mice (n=4 per group) were injected with the indicated AAV vector (1×10^{11} viral genomes/mouse) via jugular vein. (**B**) In vivo bioluminescence images obtained on 28^{th} day following vector administration. (**C**) Ex vivo bioluminescence images of the indicated tissues (heart; H, liver; L, thymus; T, kidney; K, spleen; S, intercostal muscle; Im, brain; B, Gastrocnemius; Gn,) from mice that received ACMVLuc (CMV) or AcTnTLuc (cTnT). Organs were immersed in D-luciferin solution for one minute and bioluminescence was imaged immediately thereafter using the IVIS 100 system. (**D**) Bar graph showing luciferase activities in protein extracts of the indicated tissues from the mice that received ACMVLuc (CMV) or AcTnTLuc (cTnT). Luciferase activity is expressed as relative light units per mg tissue (RLUs/mg tissue).

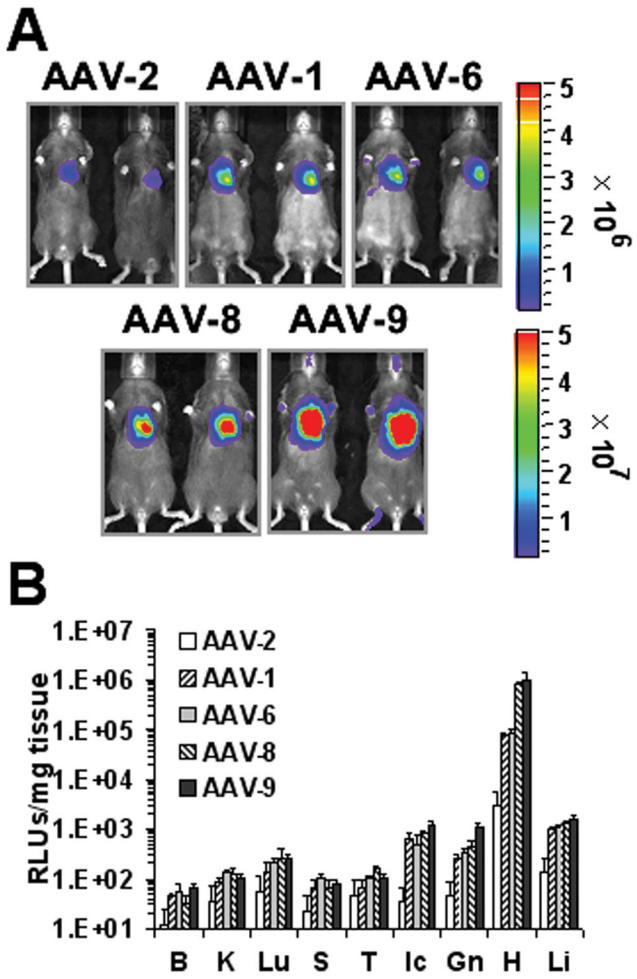

Fig. 2.

Bioluminescence imaging comparing the efficiencies of five AAV serotypes for cardiomyocyte-specific gene delivery. The AAV vector AcTnTLuc was packaged into the indicated AAV serotype capsids (AAV-2, AAV-1, AAV-6, AAV-8 and AAV-9). One week old mice (n=4 per group) were injected with 1×10^{11} viral genomes/mouse via jugular vein. (**A**) In vivo bioluminescence images obtained on day 28 after vector administration. (**B**) Bar graph showing luciferase activities in protein extracts from various tissues (brain; B, kidney; K, spleen; S, thymus; T, intercostal muscle; Im, Gastrocnemius; Gn, liver; L, heart; H) collected 28 days after vector administration. Luciferase activities are expressed as relative light units per mg tissue (RLUs/mg tissue).

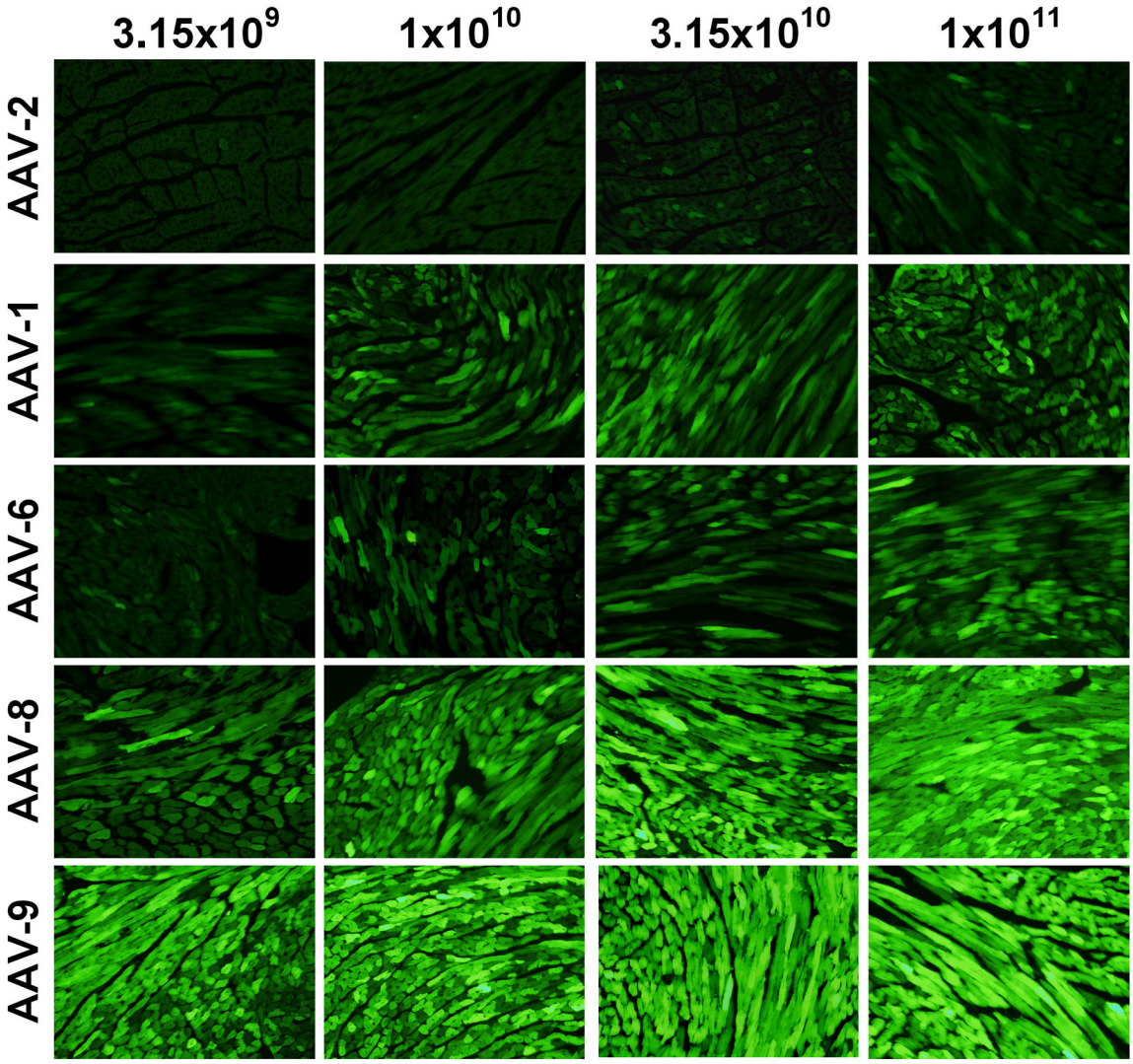

Fig. 3.

Fluorescence microscopy of heart cryosections from mice treated with increasing doses of AAV vector packaged in AAV capsid serotypes 2, 1, 6, 8, and 9. The AAV vector AcTnTeGFP was packaged into AAV capsids from the indicated serotypes (AAV-2, AAV-1, AAV-6, AAV-8 or AAV-9). One week old mice were injected with the indicated dose (n=2 per dosage) of viral genomes via jugular vein. Four weeks following vector administration, 6 μm cryosections of heart were prepared for analysis by fluorescence microscopy. All images shown here were captured at 40x magnification with a constant 0.5 sec exposure.

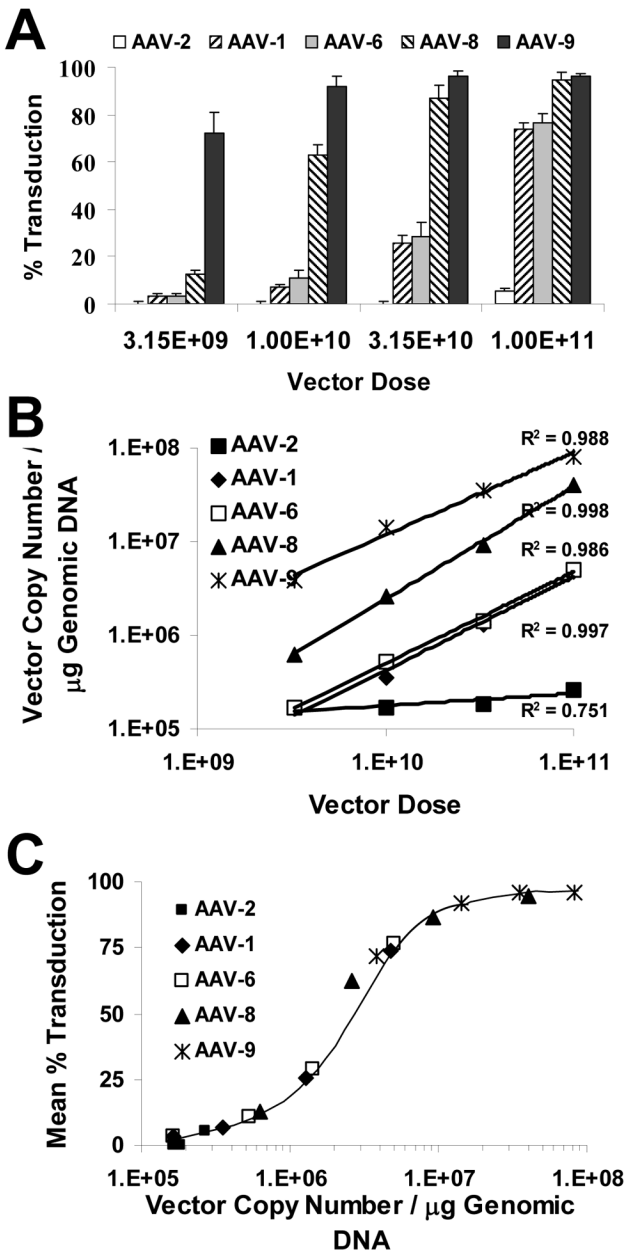

Fig. 4.

AAV vector genome copy numbers in heart following systemic administration of increasing doses of AAV vector packaged in AAV capsid serotypes 2, 1, 6, 8 and 9. (**A**) Bar graph illustrating the increase in % transduction as a function of administered dose for each of the five capsid serotypes. (**B**) Graph illustrating the linear correlation between vector dose and mean vector genome copy number per µg of genomic DNA for each of the five capsid serotypes. (**C**) Graph of percent transduction versus mean vector copy number per µg of genomic DNA illustrates the artificial plateau imposed by defining a “transduced” cell as a cell containing one of more vector genomes.

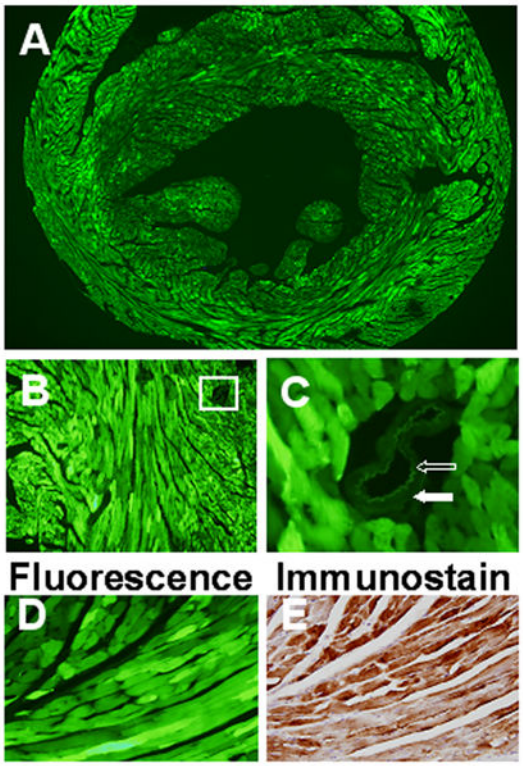

Fig. 5.

Fluorescence microscopy of heart cryosections illustrating eGFP expression. Shown are representative fluorescence images of heart cryosections from mice injected with AcTnTeGFP (AAV-9, 3.15×10^{10} viral genomes/mouse). (**A**) short-axis cross-section illustrating the homogeneity of expression throughout the extent of the left and right ventricles. (**B**) medium magnification images with the location of C indicated by white box. (**C**) 200x magnification image illustrating the lack of eGFP expression in the endothelium (open arrow) and smooth muscle cells (solid arrow) located within arterioles. (**D and E**) Comparison of eGFP protein detection by fluorescence imaging and by immunohistochemical staining. Immunohistochemical analysis was performed to confirm the eGFP expression observed by fluorescence microscopy. First, eGFP expression in the mouse heart was documented by fluorescence microscopy of heart cryosections (D). Next, after removing the coverslips, the same sections were processed for eGFP detection by immunohistochemistry (E).

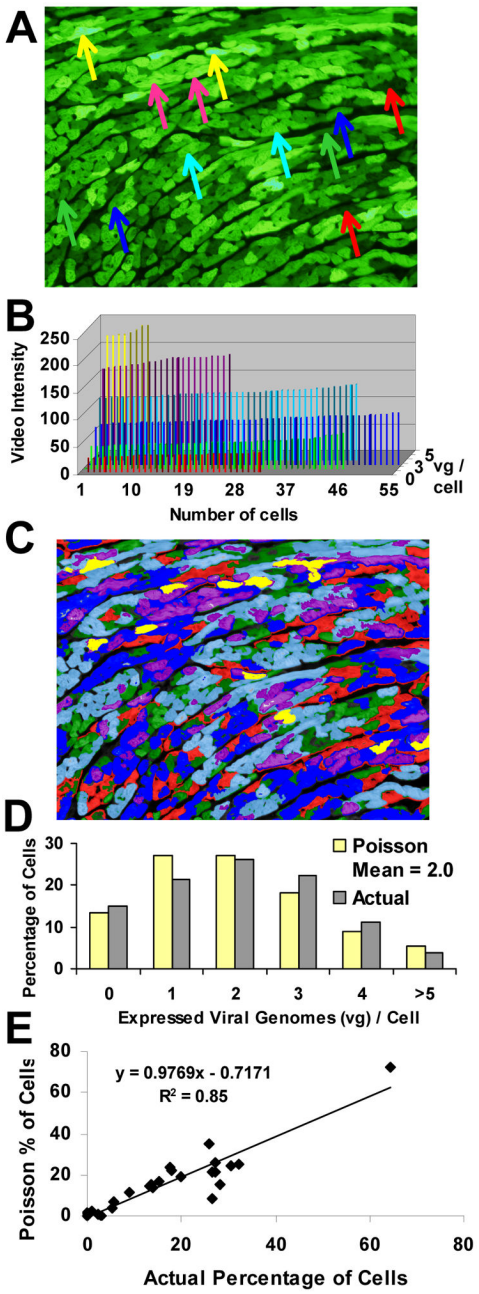

Fig. 6.

In vivo cardiac gene delivery follows a Poisson distribution. The intensity of cellular eGFP fluorescence in heart cryosections was used to assess the number of expressed viral genomes in individual cardiomyocytes. (**A**) Fluorescence image from the heart of a mouse injected with AcTnTeGFP (AAV-9, 1×10^{10} viral genomes/mouse). The tip of each arrowhead identifies a cell that was subsequently identified by K-means cluster analysis to contain n = 0 (red), 1 (green), 2 (blue), 3 (light blue), 4 (purple) and 5 or greater (yellow) AAV genomes per cell. (**B)** Three-dimensional bar graph showing the video intensities (y-axis) of individual cardiomyocytes (x-axis) from each group containing 0, 1, 2, 3, 4 or ≥5 vector

genomes (vg) per cell (z-axis) as determined by the clustering algorithm. Each bar represents a single cardiomyocyte from the FOV shown in Panel **A**. The colors red, green, blue, light blue, purple and yellow represent clusters containing 0, 1, 2, 3, 4 or ≥5 AAV genomes per cardiomyocyte, respectively. (**C**) Colorized image showing the classification of each cardiomyocyte into clusters containing n = 0, 1, 2, 3, 4 or ≥5 AAV genomes per cell, as indicated by the colors red, green, blue, light blue, purple and yellow, respectively. (**D**) Bar graph showing the percentage of cardiomyocytes expressing 0, 1, 2, 3, 4 or ≥5 viral genomes (vg) per cell determined as described in the Methods (Actual) compared to the corresponding theoretical distribution (Poisson Mean) obtained by using the mean of the actual viral genomes per cell (2.0) as the Poisson parameter (λ) = 2.0 to generate the corresponding Poisson distribution. (**E**) Correlation between the actual percentages of cells expressing "n" viral genomes (vg) as determined by image analysis and the theoretical percentages predicted by Poisson distribution. The percentages of cardiomyocytes expressing 0, 1, 2, 3, 4 or ≥5 viral genomes (vg) per cell were determined as described above (for AAV-9 at 1×10^{10} vg/mouse) as well as for AAV-9 at 3.15×10^{9} vg/mouse and AAV-8 at 3.15×10^{9} and 1×10^{10} vg/mouse (see Supplementary Information). The mean numbers of viral genomes per cell determined from image analysis were then used as the Poisson parameters (λ) to generate the theoretical distributions of percentages (as in Panel D) for both AAV-8 and -9 at both doses (3.15×10^{9} and 1×10^{10} vg/mouse). Linear regression analysis of the correlation between the actual and theoretical percentage values yielded an $R^2 = 0.85$ with a slope near unity and a y-intercept near zero, indicating a strong correlation between the empirical data and the theoretical distribution predicted by Poisson.